



SHEAR STRAIN DEVELOPMENT IN LIQUEFIABLE SOIL UNDER BI-DIRECTIONAL LOADING CONDITIONS

Annie KAMMERER¹, Jiaer WU², Michael RIEMER³, Juan PESTANA³, and Raymond SEED³

SUMMARY

A comprehensive testing database composed of modeling-quality multi-directional cyclic simple shear testing on medium to high relative density, fully-saturated samples of Monterey 0/30 sand has recently been developed. This testing program incorporated a variety of multi-directional stress paths, including a large number of stress paths never before examined. Results from these tests have proven useful for enhancing current understanding of liquefaction behavior by allowing for a more complete theory to emerge. This new 3-dimensional theory greatly expands current understanding of liquefaction behavior and elucidates some areas in which current theory—which has been based principally on uni-directional laboratory testing—can be misleading or unconservative. Of particular interest are the topics of pore pressure generation and softening, the relationship between pore pressure and strain capacity, and the dilational lock-up in medium density sands that acts to limit large free-flow type deformations. Insight has also been gained on the complex effects caused by an initial static shear stress such as would be imposed by sloping ground conditions or the presence of a structure.

INTRODUCTION

In recent years, significant research effort has been focused on developing state-of-the-art constitutive soil models capable of accurately and reliably predicting the cyclic and permanent deformations of liquefiable materials over the small to moderate strain range (<1m). Unfortunately, the use of advanced constitutive soil models for liquefiable soils is being hampered by a lack of the high-quality laboratory testing for use in the validation of existing models and development of new ones. In particular, very little modeling-quality testing has been performed on: a) liquefiable materials experiencing multi-directional stress (or strain) paths, b) medium dense to dense sand that exhibits dilative behavior with limited strain potential and c) materials under initial “driving” shear conditions as would be found in sloping ground or under a structure.

To address this need for modeling-quality data a program of simple shear testing was performed on medium to high relative density, fully saturated samples of Monterey 0/30 sand. The newly developed database that resulted is composed of two complementary series. The first consists of a comprehensive

¹ Senior Geotechnical Engineer, Arup, San Francisco, California, USA. annie.kammerer@arup.com

² Project Engineer, URS Corporation, Oakland, California, USA. jerry_wu@urscorp.com

³ Professor, University of California, Berkeley, California, USA. cegeot@ce.berkeley.edu

series of uni-directional tests incorporating several relative densities and confining pressures. In the second series, a variety of previously unexplored multi-directional stress paths were imposed. These stress paths can be separated into three general categories: bi-directional linear, oval/circular, and figure-8, as shown schematically in Figure 1. Tests were performed both with and without an initial static driving stress in order to replicate in-situ loading conditions on soils elements under both sloping and level ground conditions. This series is focused on soils that exhibit dilatant behavior (i.e. medium to high-density soils). The database is designed such that the uni-directional series serves as a comprehensive baseline against which to compare the results of the multi-directional series. Together, these series represent an unmatched resource for understanding the behavior of liquefiable soils.

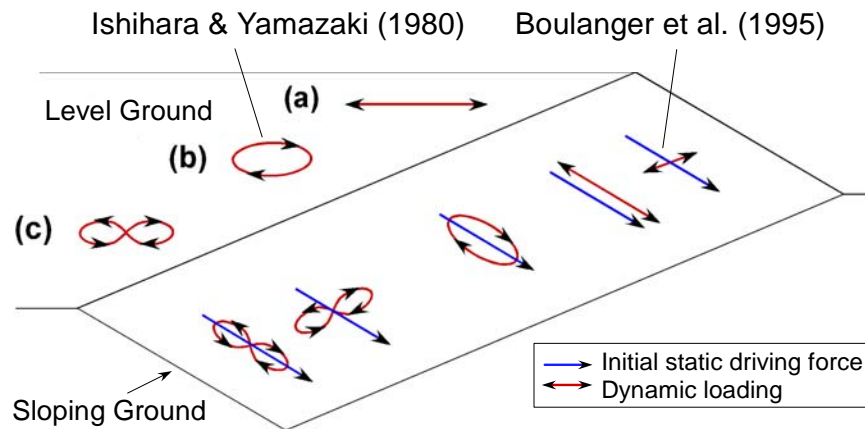


Figure 1: Schematic illustration of idealized multi-directional loading

This testing program was designed to address two ultimate goals. The first is the development of insight into the behavior of liquefiable soils under multi-directional loading conditions. The second is the development of modeling-quality laboratory data quantitatively describing the behavior of liquefiable soils for use in model development and calibration. The attainment of both goals required specialized sample preparation and testing techniques to be developed such that both the sample fabric and the imposed loading replicated typical in-situ conditions. Results from these tests have proved useful for enhancing current understanding of liquefaction behavior by allowing for a more complete theory to emerge. This new multi-directional theory greatly expands current understanding of liquefaction behavior and elucidates some areas in which the current theory can be misleading or unconservative.

This paper does not present an exhaustive discussion of the lessons that can be learned from this testing series. Instead, focus has been placed on key topics of interest. For a more complete discussion of the results of this testing program, the reader is directed to papers by Kammerer, Wu and colleagues [1, 2, 3, 4]. In addition, a companion paper in this conference describes the specifics of the database and the laboratory techniques in fuller detail [5].

LABORATORY TECHNIQUES, EQUIPMENT & MATERIAL

Testing was performed in the U.C. Berkeley Bi-directional Simple Shear Device [6], which is capable of applying horizontal shear stresses in two orthogonal directions, as well as chamber and back pressures. For this testing series fully saturated, circular, clean sand samples were constructed using wet-pluviation. The samples were contained in NGI-style wire-reinforced latex membranes that hold the sample diameter constant to assure that K_0 conditions are maintained. While this method does a good job of assuring K_0 conditions throughout the test, the actual lateral pressures applied to the testing are unknown. For the

cases where an initial horizontal static shear stress was applied to replicate sloping ground conditions (i.e. $\alpha > 0$), the horizontal stress was applied incrementally in proportion to the vertical load applied. This assured that the sample was not artificially sheared during sample preparation.

It is important to note that when developing data to be used in constitutive model development, only simple shear and torsional shear data should be used. Triaxial testing is less appropriate for this purpose as the instantaneous 90 degree rotation in the orientation of the principal stress axes is substantially different from in situ seismic loading in which a smooth rotation of the principal stress stresses occurs.

Load control was used for both the horizontal shear stresses and the vertical normal stress. This differs from the most common testing method (typically performed on dry samples) in which a constant height is maintained and the vertical load is allowed to drop. In the traditional method, the drop in vertical load is assumed to be equal to the pore pressure that would develop in a fully saturated sample. The new method used in this program allows a direct measurement of pore pressure to be recorded during testing.

Monterey #0/30 sand is a highly uniform, medium sized, sub-rounded beach sand. It was further prepared by the washing of the material over a #200 sieve to remove fine material. The D_{50} for the material is 0.36 mm, the coefficient of uniformity (C_u) is 1.29 and the coefficient of curvature (C_c), is 0.98. A minimum void ratio of 0.54 was determined by the modified Japanese method and a maximum void ratio of 0.89 was determined by the dry tipping method.

PARAMETER AND TESTING DEFINITIONS

Numerous terms and parameters have traditionally been used to describe both the state of a sample and the loading applied. However, some parameters require further specification to remove ambiguity arising from multi-directional loading and others must be newly developed. When developing new parameters and clarifying existing ones, care has been taken to assure that they can be extended to irregular loading without confusion. Several commonly used terms have been made more precise by the addition of subscripts such as “dip”, “strike”, “X”, “Y”, “max”, and “min”. The first two subscripts relate to sloping ground tests and denote the value in the direction of the initial static shear stress (or slope) and in the direction perpendicular to the initial stress, respectively, as shown in Figure 2. If no slope exists the terms “X” and “Y” can be used to differentiate the horizontal directions. The terms “max” and “min” relate to a wide variety of parameters. They can indicate the maximum direction (e.g. CSR_{max}) or the maximum absolute values within a given cycle (e.g. γ_{max}).

If common terms (e.g. shear strain (γ)) are used *without* subscripts, the magnitude of the parameter—regardless of direction—is intended. For example γ_{dip} denotes the strain in the direction parallel to the initial static shear stress, while γ denotes the largest magnitude of shear strain, regardless of the direction of the strain. It is important to note that it is the magnitude of normalized shear stress and shear strains that are presented in many of the figures provided in this paper. This is done because (1) the choice of “principal” direction is often arbitrary and (2) the data is far more meaningful when the magnitude is used. This point is stressed because the plots are similar to those the reader is likely used to and this change can potentially lead to misunderstanding, as discussed in more detail below.

Among the common definitions used in this paper are r_u , α , and CSR. The parameter r_u is the normalized pore pressure commonly defined as $\Delta u/\sigma'_c$. The α -value is the normalized initial static shear stress to which the sample has been consolidated (τ_c/σ'_c). A non-zero α -value implies that the test is replicating

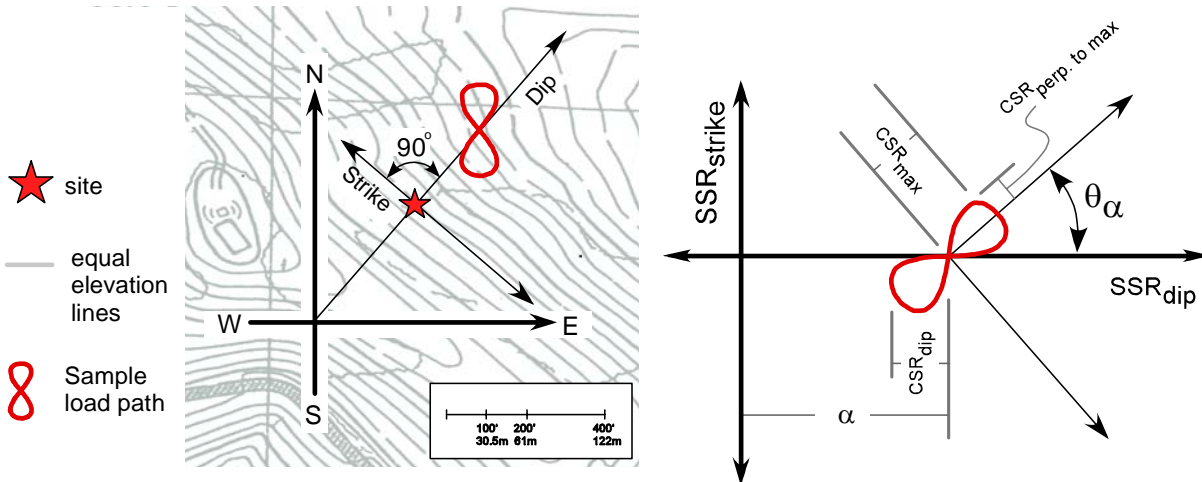


Figure 2: Multi-Directional Parameter Definitions

either the presence of a structure or sloping ground conditions during testing. This initial shear is maintained throughout testing and any cyclic load applied is, therefore, offset by this value. CSR has previously been defined as the change in normalized shear stress from the central value of the cycle. In uni-directional testing, the direction of CSR is unambiguous. However, in multi-directional testing the CSR must be defined in a specified direction and clarified with a subscript (e.g. CSR_{max} or CSR_{dip}). Examples are shown in Figure 2.

The new term, shear stress ratio (SSR), has been used in this paper to note the normalized shear stress magnitude (τ/σ'_c) at a particular point in time. Unlike the CSR, the SSR is defined at each time-step during loading (and is continually changing). Another new term is the normalized effective vertical stress. This is defined as σ'_v/σ'_c and also changes with time. This parameter is useful because (1) it allows for direct comparison of vertical effective stress and r_u at any point in a test ($\sigma'_v/\sigma'_c \approx 1-r_u$) and (2) tests with different initial vertical effective stresses can be directly compared.

MULTI-DIMENSIONAL PLOTS

There are three general categories of plots that have been developed to present the results from the bi-directional testing presented here. These are the “standard 4-way” plots, the plan view stress and strain plots, and the plan view effective stress plots. These plots are designed to present most of the same basic information currently provided for uni-directional tests, while still accommodating multi-directional loading. An example of the 4-way plot is shown in Figure 3. This series of 4 graphs are organized such that each two adjacent sets of plots have an axis in common. As a result, only four independent data series are presented. (Note that the normalized effective vertical stress is $1-r_u$. Thus these two axes are inverted.) These data series include the shear stress ratio (SSR), the normalized pore pressure ratio (r_u), the number of cycles, and the strain magnitude.

The first quadrant of the sample 4-way plot shows the magnitude of SSR (regardless of direction) and the normalized effective vertical stress. This is somewhat analogous to stress-path space commonly used in modeling. The data is presented in this form because the applied lateral stresses are unknown. However, the failure envelope is still evident in these types of plots. In addition, because the axes are of equal scale in these plots, the friction angle is also apparent. The second quadrant is the stress-strain plot. The third and fourth quadrants show the normalized pore pressure (r_u) and the shear strain (γ) as the test progresses.

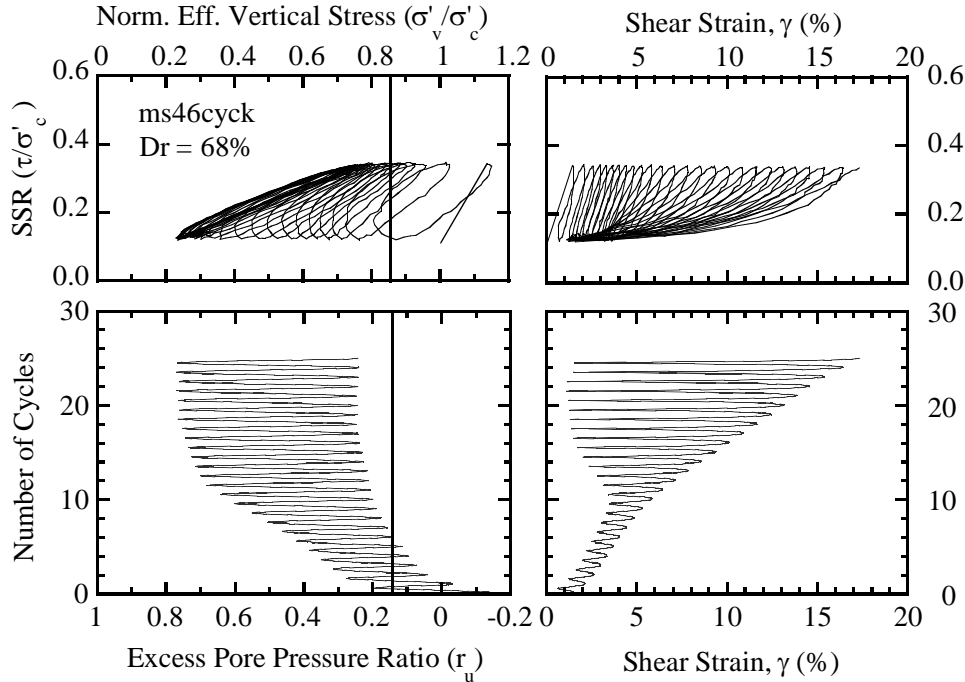


Figure 3: Standard 4-way plot for Test#Ms46cyck ($CSR_{max}=0.23$ $\alpha=0.11$)

Because strain magnitude is always positive and non-directional, this plot can not be used to determine the (single or double amplitude) strain range achieved during a given cycle. Care should be taken when viewing the 4-way and other “standard” plots that use magnitude values as misunderstandings can result. It is recommended that the reader compare the strains in Figures 3 and 4 closely. Additional discussion on this topic is provided in the companion paper [5].

The second and third category of plots used to present the data are plan view plots shown together in Figure 4. They are presented together for clarity and show the same test as in Figure 3. To allow for rapid visual assessment, the two orthogonal axes are of equal scale in each plot. The first two plots present the normalized shear stresses and strains throughout the test in plan view. The degree of both stress rotation and stress release is readily apparent in these plots. The relationship between the general stress path category and the initial static shear stress is also easily discerned by noting the location of the zero axis as compared to the center of loading. The third plot in Figure 4 shows the vertical effective stress (in plan view) throughout a single post-liquefaction cycle. The diameter of the bubble represents the value of the normalized effective vertical stress and the center of the bubble is located at the horizontal shear stresses corresponding to that point. This should be apparent when comparing the effective stress plot to the plan view shear stress plot in the same figure. The cycle shown for each of the tests is that which occurs immediately after the limiting pore pressure, $r_{u,lim}$, has been reached.

OVERVIEW OF TESTING PROGRAM

A comprehensive uni-directional test series was performed simultaneously and in conjunction with the bi-directional testing series described here in order to develop a well-verified basis from which to assess the influence of a load in a second horizontal direction (Wu et al., 2003). This testing incorporated four relative densities and three initial vertical effective stresses. The liquefaction susceptibility curves produced by this baseline series are shown in Figure 5. Triggering was defined as 3% single amplitude or 6% double amplitude shear strain. The curves for an initial vertical effective stress of 80kPa can be used

for comparison with the bi-directional series, which also incorporated a confining stress of 80kPa.

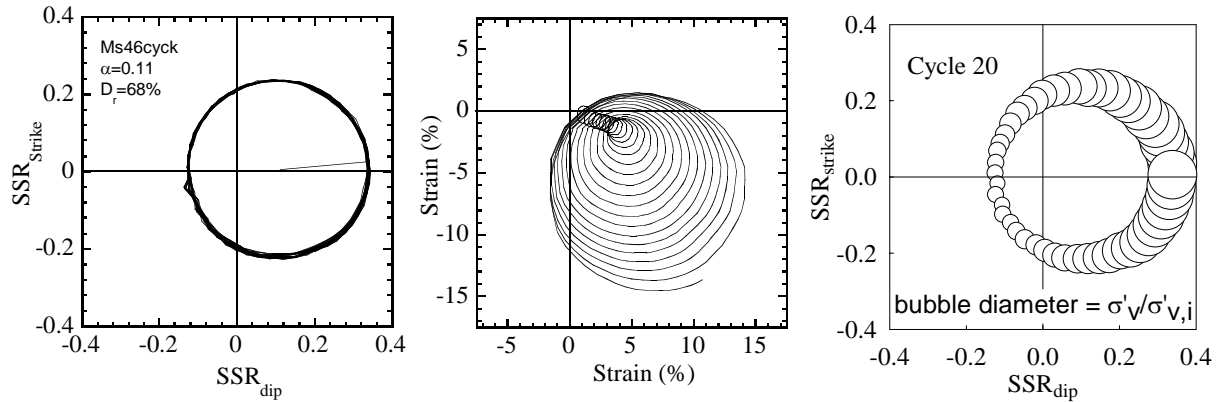


Figure 4: Plan view shear stress, strain, and effective stress plots for Test#Ms46cyck

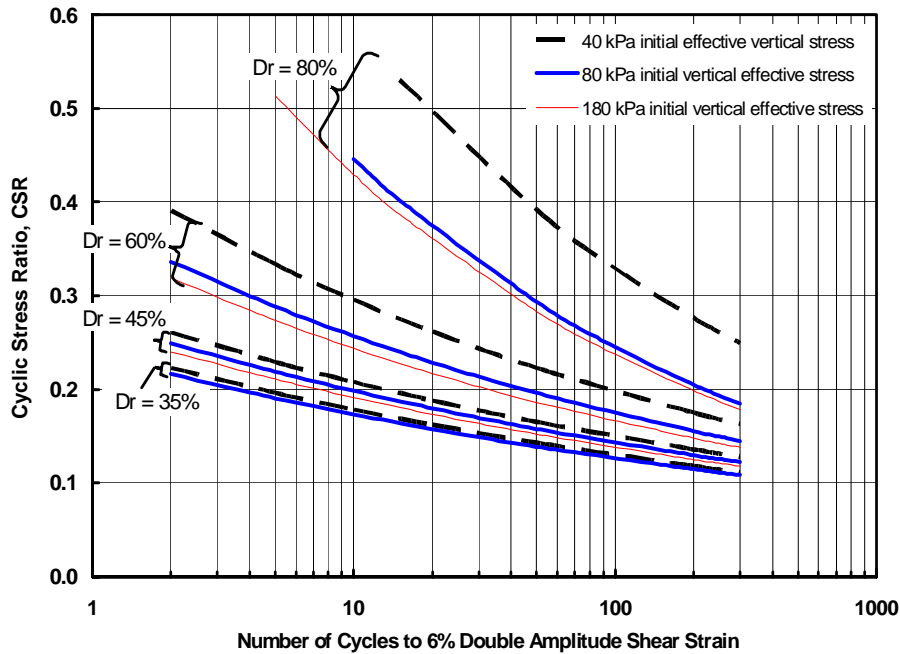


Figure 5: Liquefaction triggering curves for Monterey sand under level ground conditions

The bi-directional series performed is shown schematically in Figure 1. These stress paths can be separated into three general categories: bi-directional linear, oval/circular, and figure-8. Tests were performed both with and without an initial static driving shear stress in order to replicate in-situ loading conditions on soils elements under both sloping and level ground conditions. Additionally, the major axis of the three loading types was oriented in both the dip and strike directions for the sloping ground cases. Testing was performed at 80kPa and on medium density and high density samples. Because no additional methods were used to further densify the samples after they were built and the top cap was installed on the sample, the densities show some scatter. A range of CSR values were used. Because different stress paths had very different resistance to liquefaction, CSR values were chosen on a case-by-case basis, but

were typically 0.11, 0.22 or 0.44. Tables of the tests performed are available in the companion paper in these proceedings [5] and Kammerer et al. [1].

RESULTS

When considering the differences in behavior between uni-directional and multi-directional loading, it is useful to first recognize that there are two distinct phases in each test. The first is the period of excess pore pressure generation and accumulation, which occurs from the start of the test to the point where the failure envelope is met. During this period, the maximum pore pressure that occurs during each cycle increases until an asymptotic value is reached—after which time it shows repeated behavior during subsequent cycles. The maximum asymptotic value of the normalized pore pressure is the limiting pore pressure ($r_{u,lim}$).

The tests in Figure 6 (D, F, and G) show increasing pore pressures until a limiting pore pressure is reached, at which point the stress path plots of each cycle overlap and the maximum r_u attained in each cycle remains at its asymptotic value. Because r_u at each point is equivalent to $1-(\sigma'_v/\sigma'_c)$, the x-axes of these three plots are equivalent. Once $r_{u,lim}$ has been reached, the second phase begins. It can be noted from Figure 6 (D and G) that $r_{u,lim}$ does not necessarily reach a value of 1.0 in multi-directional tests even though large strains develop and “failure” occurs if using strain-based definitions.

Multi-directional Loading and Triggering

Not surprisingly, results from this study indicate that $r_{u,lim}$ values are typically reached more rapidly under multi-directional loading than in “equivalent” uni-directional tests (i.e. tests with the same D_r and CSR_{max}). The rotation of stresses in the horizontal plane—which occurs only in multi-directional loading—likely plays a large role in the increased rate of pore pressure development by aiding particle rearrangement and densification of the material.

When examining results, useful comparisons can often be made with similar research. However, only two previous simple shear testing programs have been conducted using regular multi-directional load paths [7, 8, 9]. The regular load paths applied in previous series are shown schematically in Figure 1. Comparisons with both these series show favorable and consistent results.

Figure 7 presents results from both the new testing program and a previous study by Ishihara and Yamazaki (1980) [7] in which they conducted tests imposing oval and circular stress paths on Toyoura sand samples. The Ishihara and Yamazaki data are shown in the plot on the right, which indicates the number of cycles to failure for level ground tests with a variety of aperture ratios (AR), as it is defined in Figure 7. An AR of 0 is a uni-directional test, an AR of 1 denotes a circular load path, and intermediate values denote ovals. The leftmost plot presents results from the new testing series. The curve for AR=0 is estimated from the triggering shown in Figure 5 for a relative density of 65%. Also shown are results from individual oval and figure-8 tests (AR=0.5) and circular tests (AR=1).

These studies indicate similar trends in behavior, even though the sands, relative densities, and initial confining stresses used in the two studies differ significantly. The trends include a general decrease in liquefaction resistance with both an increased aperture ratio (AR) and increased cyclic stress ratio (CSR_{max}). Both studies also show a similar reduction in additional effect as the aperture ratio increases.

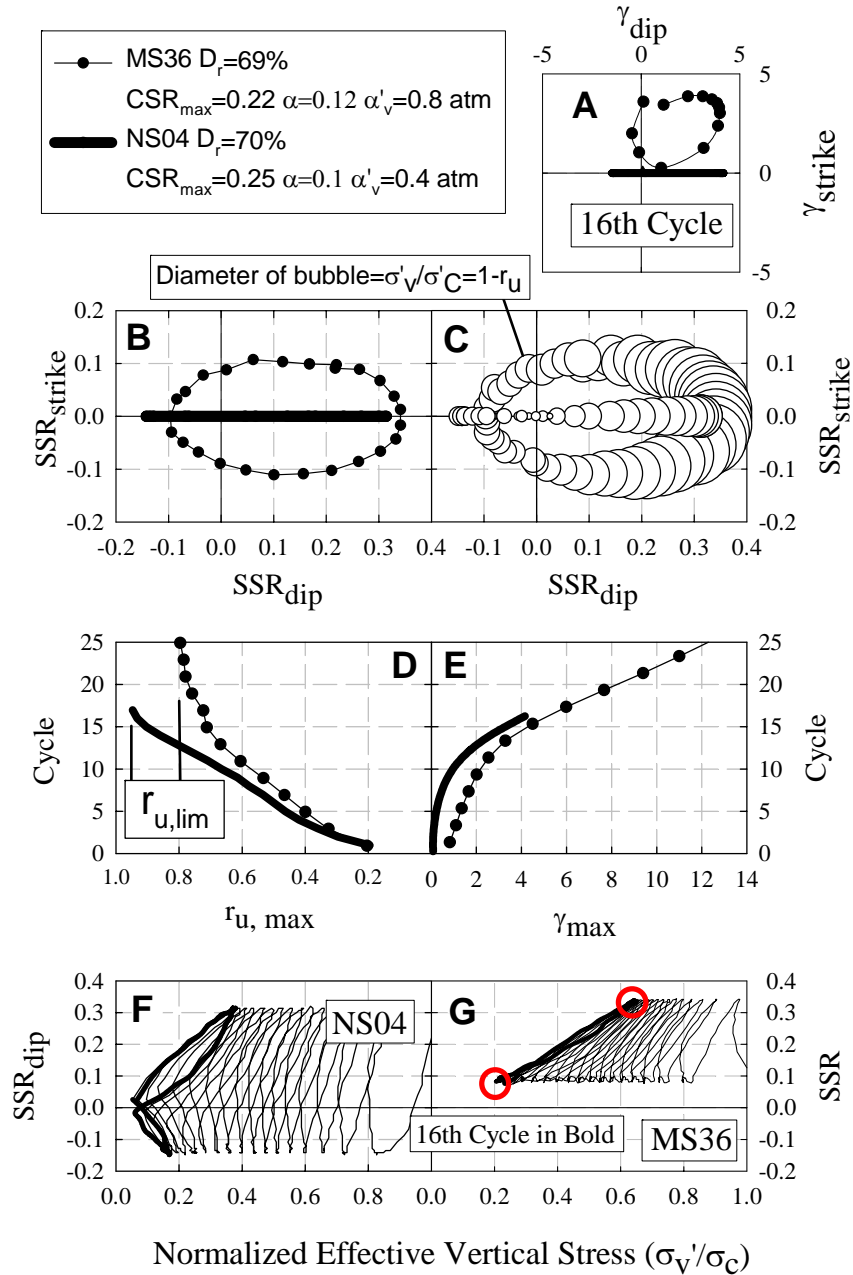


Figure 6: Comparison Between Linear And Oval Tests

While the general behavior of the samples tested under typical CSR values are consistent, the behavior of some tests (42k, 44k, and 68k) is somewhat unexpected. Unlike in the study by Ishihara and Yamazaki this research found that in some cases the application of a second direction of loading could be detrimental. These are tests with very high CSR_{max} values that are expected to fail within a cycle or two. The reason for this seemingly counter-intuitive behavior is discussed in more detail in the following sections. While the effect of a second horizontal loading direction in these oval/circular tests seems relatively well behaved, the impact across loading categories—particularly those incorporating sloping ground—is harder to simplify and model. Research to develop quantitative rules for pore pressure generation under multi-directional loading is ongoing.

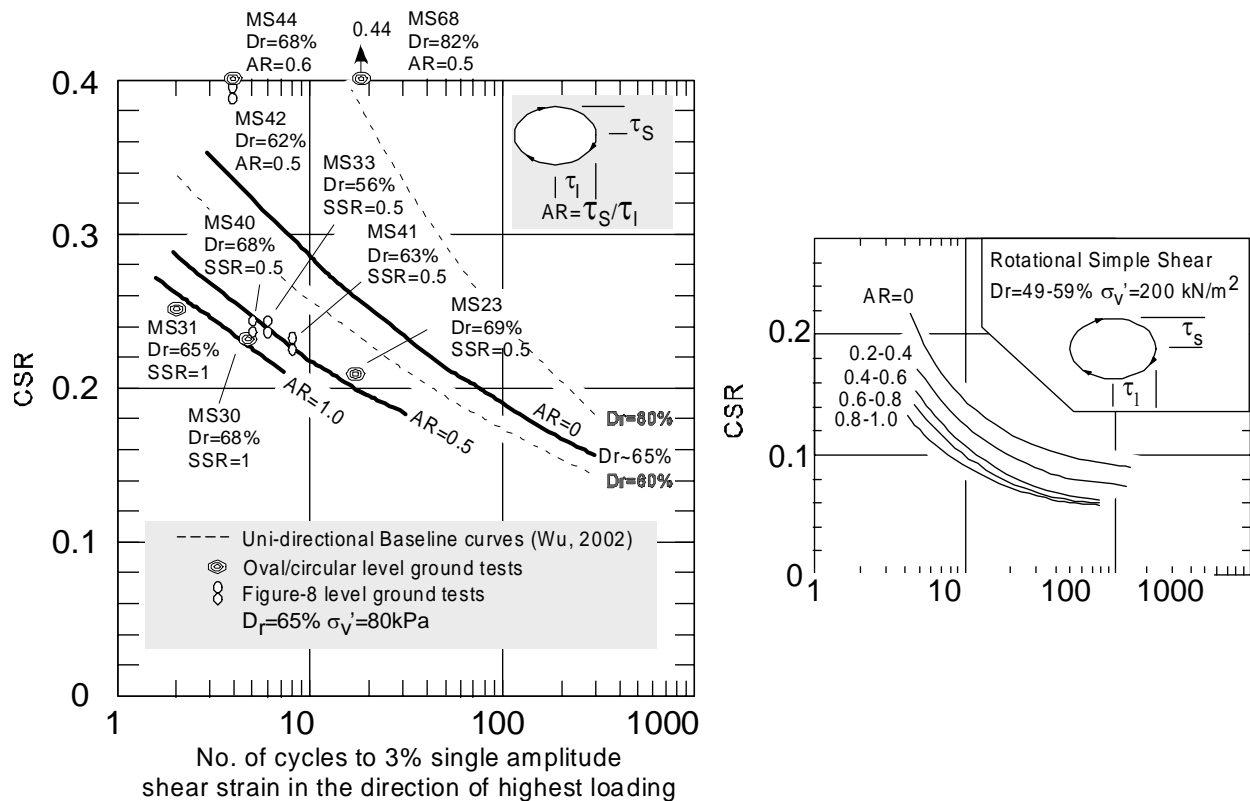


Figure 7: Comparison of results from this study (left) and Ishihara and Yamazaki, 1980 (right) and for level-ground tests

The Effect of Initial Static Shear Stress on Pore Pressure Generation, and Strains

As in uni-directional testing, a sufficiently large initial static shear stress ratio (i.e. high α) can decrease the potential for excess pore pressure generation by eliminating shear stress reversal and keeping the grains locked together. Unlocking of soil grains in uni-directional loading requires not only the removal of shear stresses, but also some loading in the uphill direction. In the past, tests with very small amounts of stress reversal have shown the same limited behavior as tests with no stress reversal [9, 10, 11].

Very high α -values can also prevent liquefaction in multi-directional tests, though the α -values required may be much larger than for the equivalent uni-directional tests, depending on the stress path. Figure 8 examines the importance of stress reversal and rotation in multi-directional tests by comparing tests with similar CSR_{max} values and degrees of stress reversal in the dip (downhill) direction, but with different orientations. There are two tests with different densities shown for each orientation. In this series one set of tests has a much higher degree of rotation, while the other has a much higher maximum shear stress.

The dip-oriented tests have an α -value that results in limited stress rotation and no stress reversal in the dip direction. The reduced pore pressure generation and strain development in these tests compared to the strike-oriented tests is apparent, although some limited shear strains develop due to the minor rotation that does occur. This can be contrasted with uni-directional tests for which almost zero straining would be likely.

The strike-oriented tests showed both larger cyclic and larger permanent strains due to the higher stress rotation, even though the maximum shear stresses imposed on the samples were lower than in the dip-

oriented tests. For this set of test conditions, the amount of shear stress reversal/rotation was more important than the maximum shear stress imposed. The shear strains recorded in the strike-oriented tests show larger permanent downhill movement than cyclic straining, even though the cyclic loading is much larger than the initial static driving shear stress. It is almost universal in sloping ground tests that the principal straining is in the downhill directional regardless of the orientation of the loading that leads to softening. One may note that there are also permanent strains in the strike direction. Though the loading seems symmetric, each time the highest pore pressure (and highest degree of softening) is achieved, the load path is moving in the same counter-clockwise direction.

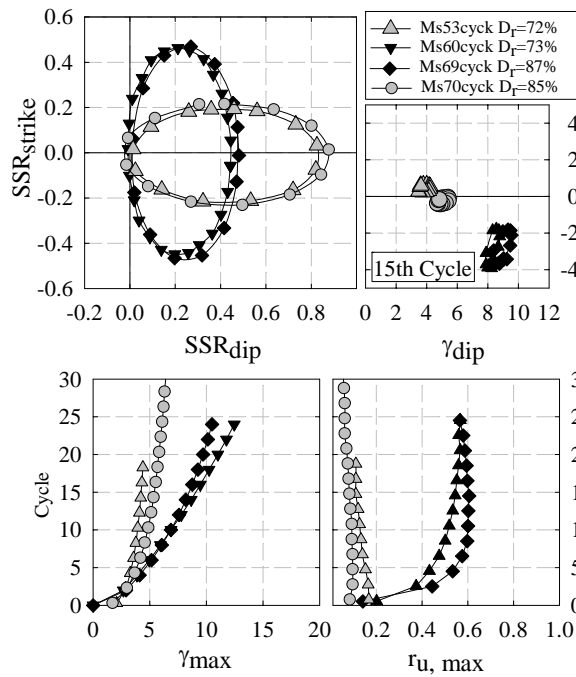


Figure 8: Comparison of dip and strike-oriented oval oriented tests with increasing α -values

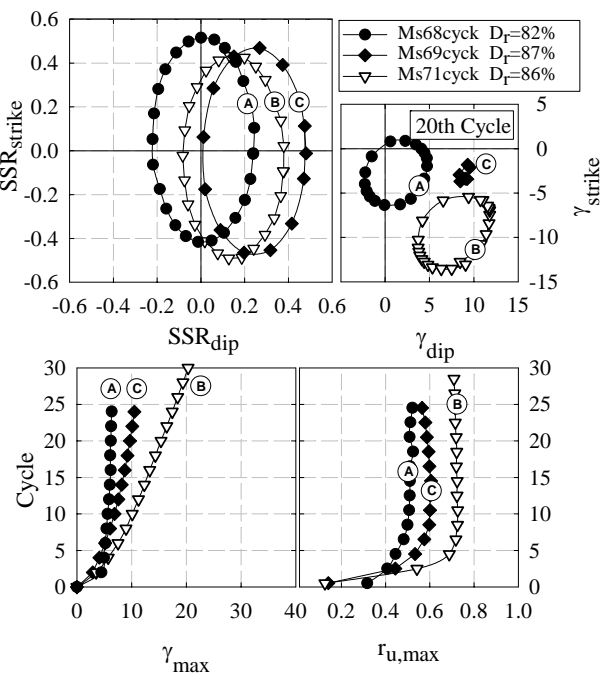


Figure 9: Comparison of dip-oriented oval tests with increasing α -values

Figure 9 shows three strike-oriented oval tests with increasing α -values. Clearly, the initial load has a large effect on the magnitude and type of strains achieved. The test with no stress reversal in the dip-direction (c) showed the least cyclic deformation, though the permanent strains were high. The level-ground oval test (a) showed larger cyclic movements, but little permanent deformation. The test with the moderate α -value (b) produced the largest strains, both cyclic and permanent, because the sample both experienced a 360-degree rotation and had a driving shear stress in the dip direction throughout loading. Again the effect of the directionality of loading is apparent. In addition, it can be seen that many tests produce large deformations, while maximum normalized pore pressure values remain well below 1.0.

The Relationship between Shear Stress and Post-Triggering Pore Pressure Behavior

Once the limiting pore pressure ($r_{u,lim}$) has been achieved in a given test, the pore pressures measured throughout each cycle of uniform loading show repetition of behavior. Fig 10 shows the limiting maximum and limiting minimum pore pressures ($r_{u,lim}$ and $r_{u,lim,min}$) for each liquefied test in the series plotted against the shear stress ratios at which each of these values occurs. The parameter $r_{u,lim,min}$ is defined as the minimum pore pressure that occurs in a test with regular loading after $r_{u,lim}$ has been achieved. As an example, the $r_{u,lim}$ and $r_{u,lim,min}$ values plotted for tests MS36cyck are highlighted by the circles on Figure 6 (G). This limiting pore pressure data exhibits a roughly linear relationship with shear

stress. The few values that plot noticeably below the trend lines are cases where there was no shear stress reversal in the dip direction, but where the sample still liquefied due to large shear stresses in the strike direction (e.g. tests MS60k MS89k in Figure 8). In addition, samples that do not soften would plot at much lower pore pressures than would be expected from this relationship.

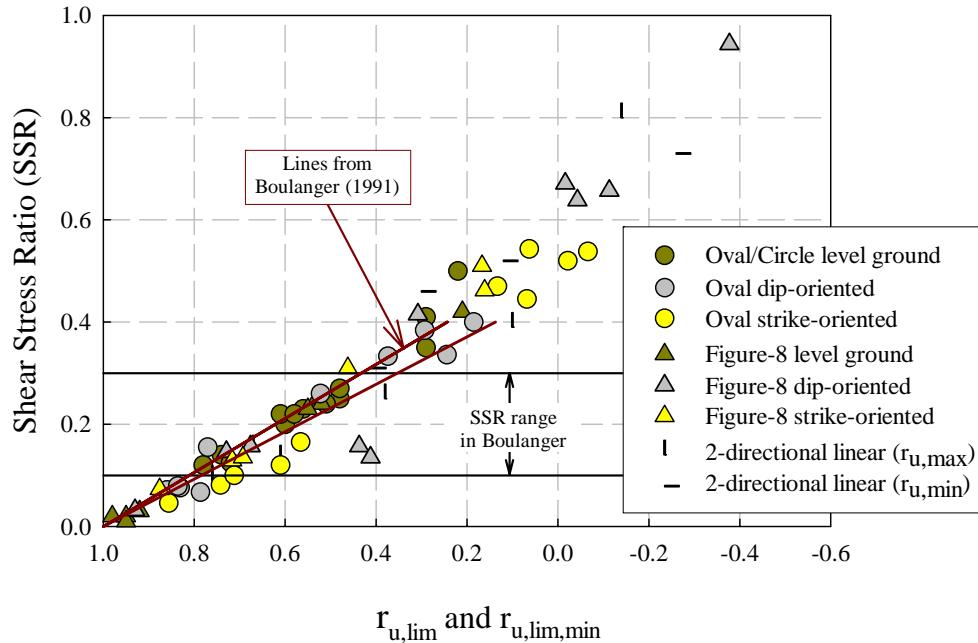


Figure 10: Normalized maximum and minimum pore pressure values during a “liquefied” cycle as a function of the shear stress ratio

These results are consistent with those obtained in an earlier program by Boulanger and Seed [8]. This earlier testing series on Sacramento River Sand used a linear stress path that included an initial static driving shear stress (i.e. $\alpha > 0$) and was oriented in the strike direction, as shown in Figure 1. The lines from this earlier program (as shown on Figure 10) bound the plots of $r_{u,lim}$ versus α for the tests performed. Because α was equivalent to SSR_{min} in this series, a direct comparison can be made.

This inverse relationship between shear stress and post-triggering pore pressure can be explained by considering dilation of the soil particles. In both uni- and bi-directional tests, dilation causes a drop in pore pressure as limiting strains are reached and particles are forced to move over each other. In the case of uni-directional loading, this relative motion must occur within a single plane. In multi-directional loading there is more freedom of movement, making the resulting dilation less problematic but still evident.

There are also cases, however, when the drop in pore pressure due to shear stress is large enough that the soil cannot soften or softens more slowly than expected. This occurs with certain load paths in which the shear stresses imposed remain very large. Examples of this are Tests MS42cyck, MS44cyck and MS68cyck in Figure 8. The linear relationship between SSR and r_u is foreseeable because the values plotted are principally located on the failure envelope for each test. For example, in Figure 6 (G) every point of the final cycle remains on the failure envelope. It is only during unloading in some stress paths that the stress state of the sample does not plot on the failure plane due to a lag in the pore pressure [4].

The Relationship between Shear Stress and Post-Triggering Strain Behavior

As shown in Figure 10, the excess pore pressure shows a reverse-linear relationship to the shear stress imposed at any point along a stress path. However, because the shear stress itself also acts as a driving stress, two conflicting effects are occurring at each point in a given stress path. The results of this research indicate that there is a range of shear stresses for which the balance between these two competing behaviors result in high shear strain potential, as shown schematically in Figure 11.

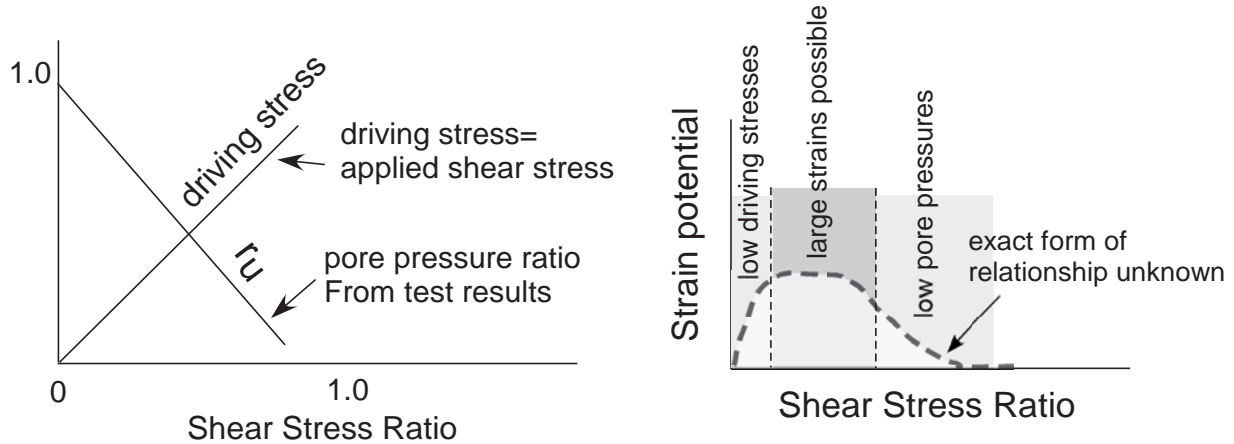


Figure 11: Relationship between pore pressure generation and driving shear stress

Consider that for very small values of shear stress, the pore pressures are high and the sample is softened to a large extent, but the driving stresses that deform the sample are low. In the very high shear stress region, the driving stresses are high, but the pore pressure is reduced to a value below which softening can occur. In some region of moderate shear stresses, reasonable driving stresses are present but pore pressures are still adequate for softening. This results in a range of SSR values with high strain potential.

Figures 12 and 13 present examples of test series in which this optimal shear stress range for high strain potential is evident. In both these series, it is not the sample with the highest CSR that shows the largest strains, but rather samples experiencing more moderate shear stresses. These tests are particularly useful in understanding this phenomenon because there is a smaller range of shear stresses applied to these samples than in other shear stress paths. This limited range allows for a simpler, clearer picture to emerge. It should be noted that all six tests in these figures exhibit large strains that would be considered “failure” of the sample.

This balance between pore pressure generation and driving stress has not been recognized widely in the past, if at all. In fact, these results seem at the surface to contradict other testing that has found that for soils loaded under level-ground one-directional conditions, an increase in loading level (CSR) always decreases the number of cycles required to achieve “failure”. However, this is easily explained because in uni-directional level-ground testing the shear stresses necessarily range from zero to SSR_{max} twice in each cycle, thus there is little chance of recognizing or differentiating any region of higher shear strain potential. By contrast, in multi-directional testing it is possible to test a sample with a very only a very small range of shear stresses. For example, the test shown in Figure 4 has a more limited stress range than a uni-directional tests. A level-ground circular test has only a single shear stress magnitude.

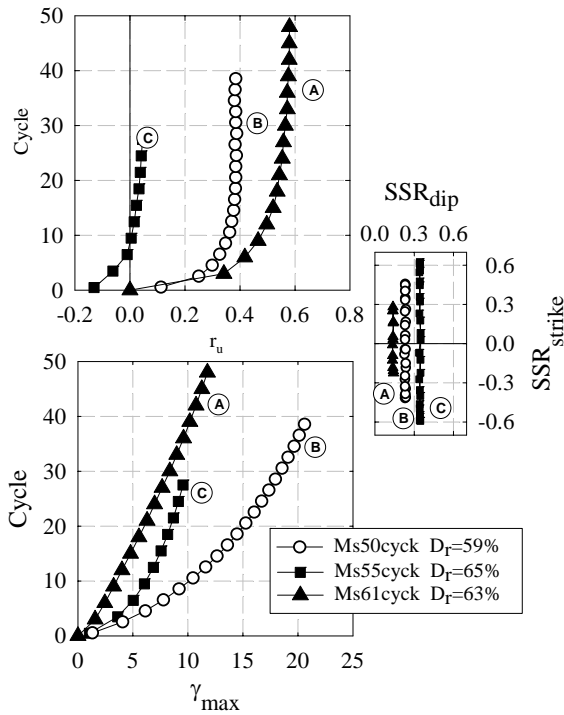


Figure 12: Comparison of strains in bi-directional linear tests

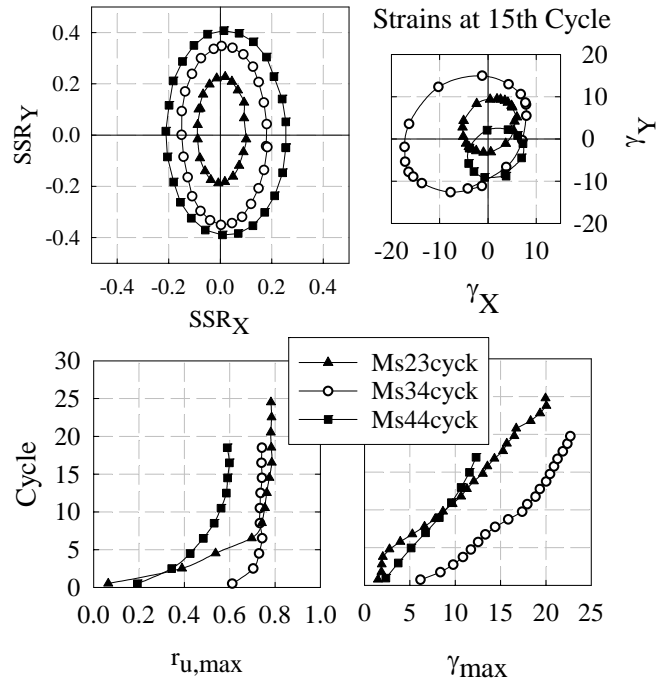


Figure 13: Comparison of strains in level-ground oval tests

An Illustrative Comparison of Complex Behaviors

Figure 14 shows three dip-oriented figure-8 tests with increasing α -values. These tests exhibit a variety of interesting behaviors. Clearly the strains of the three tests differ significantly. In the test with the highest driving shear stress, no stress reversal occurs in the dip direction. This is similar to the dip-oriented oval tests in Figure 8. In fact, both the loads and strains are similar between these two load paths. The minor difference in these two load paths does not appear to significantly impact the test behavior.

The level ground test in Figure 14 (ms42cyck) exhibits cyclic deformations as expected, but it also moves in the lateral direction due to lack of symmetry of the load path in that direction. Every time the sample approaches the point of zero shear and highest softening, it is moving in the same direction, leading to permanent displacement. The test with the moderate α -value of 0.2 is most influenced by the portion of the load cycle in which the rotation about the point of zero shear stress occurs. It is clear when looking at the strains recorded that for part of the load path the shear stresses imposed on the sample lower the pore pressure to a point where the sample is no longer softened. Strains are inhibited in this portion of the load path. To examine the effect of this further, a circular test was performed which approximated the stresses of the low-stress half of the figure-8 test. In this circular test, the loads were not sufficient to cause liquefaction. This indicates that although the high stress portion of the path does not contribute to strains, it does contribute to initial triggering.

In addition, the relationship between shear stress and post-triggering pore pressure can also be seen in the effective stress plots of this figure. It is perhaps clearest with the upper most test, which approaches zero effective stress near the point of zero shear stress (at the origin) and increases as the loads are again applied. The relationship is also visible in the other two tests, though the pore pressures in the bottom test are lower than expected due to limited softening.

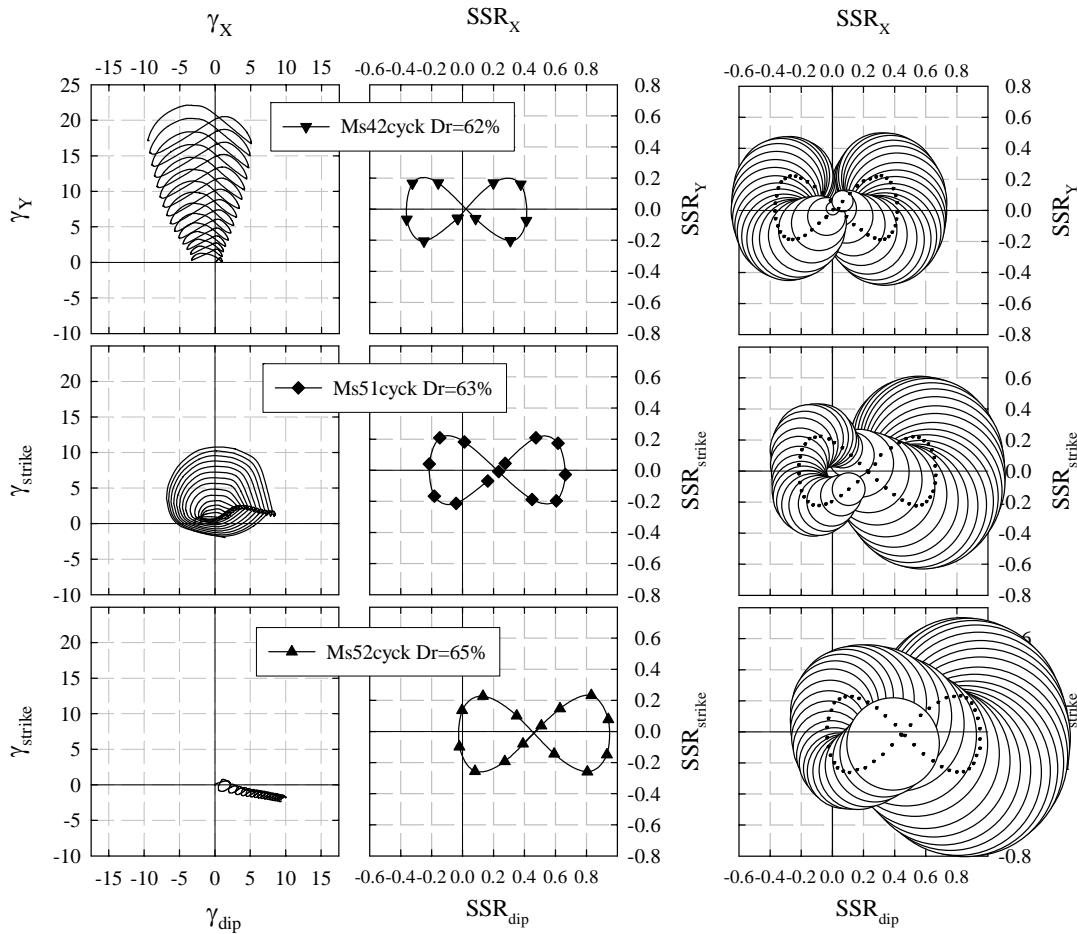


Figure 14: Comparison of dip-oriented figure-8 tests

SUMMARY

While the behavior of liquefiable soils under multi-directional loading is far too complex to fully address here, the general behaviors discussed in this paper can be summarized.

- The addition of shear stress in a second horizontal direction tends to result in quicker attainment of $r_{u,lim}$. The biggest change in liquefaction resistance occurs when the load is first applied in the second direction. Further increase in this perpendicular load continues to lower triggering resistance, but with declining effect.
- After the limiting pore pressure ($r_{u,lim}$) has been achieved in a given test, the pore pressures measured at any point during a cycle show a (roughly) linear relationship with the shear stress at that point. This relationship can be estimated from the failure envelope, though some exceptions do apply.
- There is a range of shear stress values where the balance between driving stress and pore pressure development lead to high strain potential.
- The assumption that the excess pore pressure within a sample must approach the total vertical stress (resulting in $r_u \approx 1.0$) in order for “liquefaction” to be achieved must be reassessed based on results showing that a large number of tests exhibited large strains with relatively low maximum pore

pressures ($r_{u,max}=0.7$ or less). This logically follows once it is recognized that (a) there is a relationship between minimum shear stress and maximum excess pore pressure and (b) few multi-directional tests experience points of zero shear stress.

- The presence of an initial static driving shear stress, as would be found under a sloping ground site or a structure, has a strong influence on shear strain development. Moderate shear strains tend to have the highest strain potential. At sites with a very high initial shear stress, loading may not be large enough to allow for shear strain reversal. When this occurs softening is limited. Unlike in uni-directional tests, however, even a very small load in the uphill direction can have a very large impact on softening.

ACKNOWLEDGEMENTS

Support for this research was provided by the NSF, CAREER award CMS-9623979, by the Pacific Earthquake Engineering Research Center (project 2051999), by a National Science Foundation Graduate Research Fellowship and an EERI/FEMA NEHRP Graduate Research Fellowship. On-going support for publication and presentation provided by Ove Arup and Partners California, Ltd. (ARUP)

REFERENCES

1. Kammerer, A.M, Pestana, J.M. and Seed, R.B. (2002) "Undrained Response of Monterey 0/30 Sand Under Multidirectional Cyclic Simple Shear Loading Conditions", Geotechnical Engineering Research Report No. UCB/GT/02-01, University of California, Berkeley, July 2002.
2. Wu, J., Seed, R.B. and Pestana, J.M. (2003) "Liquefaction Triggering and Post Liquefaction Deformations of Monterey 0/30 Sand under Uni-Directional Cyclic Simple Shear Loading", Geotechnical Engineering Report No. UCB/GE-2003/01, April 2003, UC, Berkeley
3. Wu, J., Kammerer, A.M., Riemer, M.F., Seed, R.B., and Pestana, J.M.(2004), "Laboratory Study of liquefaction triggering criteria", Proceedings, 13th World Conf. on Earthquake Engr., Paper 2580, Vancouver, Canada,
4. Kammerer, A. M., Seed, R.B., Wu J., Riemer M. F., and Pestana J. M. (2004) "Pore Pressure Development in Liquefiable Soils Under Bi-Directional Loading Conditions", Proceedings, 11th Int. Conf. on Soil Dynamics and Earthquake Engineering, Vol.2 P.697
5. Kammerer, A.M., Wu, J., Riemer, M.F., Pestana, J.M., and Seed, R.B.(2004), "A New Multi-Directional Direct Simple Shear Testing Database", Proceedings, 13th World Conf. on Earthquake Engr., Paper 2083, Vancouver, Canada
6. Boulanger, R. W., Chan, C. K., Seed, H. B., and Seed, R. B. (1993). "A low-compliance bi-directional cyclic simple shear apparatus." Geotech. Testing J., 16(1), 36-45.
7. Ishihara, K. and Yamazaki, F. (1980). "Cyclic simple shear tests on saturated sand in multi-directional loading." Soils and Foundations, 20(1), 45-59.
8. Boulanger, R. W. and Seed, R. B. (1995). "Liquefaction of sand under bi-directional monotonic and cyclic loading." J. Geotech. Engng., ASCE, 121(12), 870-878.
9. Boulanger, R. W., Seed, R. B., Chan, C. K., Seed, H. B., and Sousa, J. B. (1991). "Liquefaction behavior of saturated sands under uni-directional and bi-directional monotonic and cyclic simple shear loading." Rep. No. UCB/GT-91/08, University of California, Berkeley.
10. Harder, L. F. and Boulanger, R. W. (1997). "Application of $K\sigma$ and $K\alpha$ Correction Factors." Rep. No. NCEER-97-0022, NCEER, Buffalo.
11. Vaid, Y. P. and Finn, W. D. L. (1979). "Static shear and liquefaction potential." J. Geotech. Eng. Div., ASCE, 105 (GT10), p.1233